

# **CFD SIMULATION TO STUDY THE EFFECTS OF RIBS IN A CONVERGING NOZZLE FLOW AT SONIC MACH NUMBER**

**AMBAREEN KHAN**

**UNIVERSITI SAINS MALAYSIA**

**2020**

**CFD SIMULATION TO STUDY THE  
EFFECTS OF RIBS IN A CONVERGING NOZZLE  
FLOW AT SONIC MACH NUMBER**

by

**AMBAREEN KHAN**

**Thesis submitted in fulfillment of the requirements  
for the degree of  
Master of Science**

**April 2020**

## **ACKNOWLEDGEMENT**

First and foremost, All Praises be to Allah the Almighty for delivering me the patience, the potency, and the guidance to conclude this thesis fruitfully.

I would like to express my sincere gratitude and appreciation to my supervisor, Associate Professor Dr. Nurul Musfirah Mazlan, for her guidance, support, and motivation and, above all, to offer me the opportunity by accepting me as a Master student.

I owe the highest debt to my father, mother, and husband and all brother for not only their never-ending affection, love, and patience, but also their encouragement and unconditioned support to me in all my decisions. Their guidance helped me to keep my motivations high throughout my studies. In addition to this, the help and support from my Husband (Dr. Mohammad Nishat Akhtar) to accomplish this degree was admirable. He has always motivated me in all aspects of my life.

I would also like to thank my co-supervisor, Mohd. Azmi Ismail for his guidance and support and all technical and non-technical staff of Aerospace School for their guidance during the course of my study.

I would like to give special thanks to my father and Professor Asif, for their full support and knowledge in my research.

# TABLE OF CONTENTS

<b>ACKNOWLEDGEMENT.....</b>	<b>ii</b>
<b>TABLE OF CONTENTS.....</b>	<b>iii</b>
<b>LIST OF TABLES.....</b>	<b>v</b>
<b>LIST OF FIGURES.....</b>	<b>vi</b>
<b>LIST OF SYMBOLS.....</b>	<b>ix</b>
<b>LIST OF ABBREVIATIONS.....</b>	<b>xi</b>
<b>ABSTRAK.....</b>	<b>xii</b>
<b>ABSTRACT.....</b>	<b>xiv</b>
<b>CHAPTER 1 INTRODUCTION.....</b>	<b>1</b>
1.1 Background.....	1
1.2 Problem Statement .....	2
1.3 Research Gap.....	4
1.4 Objectives of Research.....	4
1.5 Scope of the Study.....	5
1.6 Contributions of this Research.....	6
1.7 Thesis Outline.....	6
<b>CHAPTER 2 LITERATURE REVIEW.....</b>	<b>8</b>
2.1 Characteristics of Backward Facing Step.....	8
2.1.1 Shear Layer.....	9
2.1.2 Coherent Structures.....	10
2.1.3 Reattachment Zone.....	11

2.1.4	Recirculation Zone.....	11
2.2	Passive Control.....	14
2.2.1	Application of Passive Control in Different Type of Flow.....	14
2.2.2	Advantages of Passive Control.....	20
2.2.3	Disadvantages of Passive Control.....	21
2.3	Summary.....	21
<b>CHAPTER 3 METHODOLOGY.....</b>		<b>23</b>
3.1	Introduction.....	23
3.2	Governing Equations Related to the Simulation.....	24
3.3	Boundary Conditions.....	27
3.4	Mesh Independence Check.....	28
3.5	Validation of Simulation Work.....	29
3.6	Set-up for Duct of Diameter, D=25 mm.....	32
3.7	Set-up for Duct Diameter, D=20 mm.....	34
<b>CHAPTER 4 RESULTS AND DISCUSSION.....</b>		<b>36</b>
4.1	Comparison between Single, Multiple and Without Ribs for Area Ratio 6.25.....	36
4.2	Effect of Location of Rib in the Duct for Area Ratio 6.25.....	40
4.3	Effect of NPR on Base Pressure for Area Ratio 6.25.....	46
4.4	Effect of Aspect Ratio and Location of the Rib for Area Ratio 4.....	54
<b>CHAPTER 5 CONCLUSION.....</b>		<b>62</b>
5.1	Recommendations for Future Work.....	63
<b>REFERENCES.....</b>		<b>64</b>
<b>APPENDIX</b>		

## LIST OF TABLES

	<b>Page</b>
Table 2.1 Types of Flow.....	13
Table 3.1 Boundary Conditions.....	27
Table 3.2 Summary of Various Flow Parameters Combinations Investigated.....	28

## LIST OF FIGURES

		<b>Page</b>
Figure 1.1	Backward Facing Step.....	1
Figure 1.2	Suddenly Expanded flow.....	5
Figure 2.1	Flowfield at Backward Facing Step.....	9
Figure 2.2	Jet-Pump action.....	13
Figure 2.3	(a) Convergent nozzle, (b) enlarged duct and (c) annular ribs with wooden holder.....	16
Figure 2.4	Nozzle and duct dimensions.....	17
Figure 3.1	Flowchart for the layout of research.....	24
Figure 3.2	Three different element size having converged values.....	29
Figure 3.3	Duct with 5 ribs used by Rathakrishnan.....	30
Figure 3.4	Geometry of Duct with 5 ribs used by Rathakrishnan.....	30
Figure 3.5	Geometry Mesh (a) Mesh of the geometry and (b) Close-up look to the Mesh.....	30
Figure 3.6	Comparison of experimental and numerical results.....	32
Figure 3.7	Nozzle and duct arrangement with rib.....	33
Figure 3.8	(a) Mesh of the Single Rib geometry for aspect ratio 3:3 at 3D location (b) A close look of the mesh around the rib.....	34
Figure 3.9	Nozzle and duct arrangement with rib.....	34
Figure 3.10	(a) Mesh of the geometry of duct, D=20 mm for aspect ratio of the rib 3:1 at 2D location (b) A close look of the mesh near the rib.....	35
Figure 4.1	Velocity contours, streamlines, and view of recirculation zones of the flow field in the duct with no ribs, single rib, and multiple ribs.....	39

Figure 4.2	Base pressure variation with ribs (rib aspect ratio 3:3, NPR = 2.5).....	40
Figure 4.3	Base pressure concerning increasing aspect ratio (3:1 to 3:5) at different duct positions.....	42
Figure 4.4	Streamlines showing recirculation zones.....	44
Figure 4.5	Pressure distribution for different rib position.....	46
Figure 4.6	Fall and Rise of the base pressure for aspect ratios from 3:1 to 3:5 of single rib at a 3D location and NPR from 1.5 to 5 compared to smooth duct having no rib.....	48
Figure 4.7	Change inflow velocity pattern and its increase with NPR, particularly at the rib location having W:H = 3:3.....	50
Figure 4.8	Influence on flow velocity vectors at different aspect ratios at NPR 2.5 .....	51
Figure 4.9	At NPR 2.5 (a) Smooth wall pressure and axial pressure in the duct with no rib (b) Fluctuating wall pressure and axial pressure in the presence of rib.....	52
Figure 4.10	Turbulent kinetic energy variation obtained from k-equation model....	53
Figure 4.11	Turbulence eddy dissipation with an increase in NPR.....	54
Figure 4.12	Increase in base pressure with rib location and its aspect ratio.....	57
Figure 4.13	Pressure distribution for different rib location of aspect ratio 3:1.....	57
Figure 4.14	Pressure distribution for different rib location of aspect ratio 3:2.....	59
Figure 4.15	Pressure distribution for different rib location of aspect ratio 3:3.....	59
Figure 4.16	Base pressure changes when NPR is increased from 1.5 to 5, and the	



aspect ratio is changed from 3:1 to 3:3.....60

Figure 4.17 Iso-lines of velocity ( $u$ ) in the duct with no rib and rib having a  
different aspect ratio.....61

## LIST OF SYMBOLS

$M$	Mach Number
$P_a$	Ambient/atmospheric Pressure
$P_e$	Pressure at the exit of the nozzle
$\rho$	Density
$\mu$	Viscosity
$\mu_o$	Reference Viscosity
$T$	Static Temperature
$T_o$	Reference Static Temperature (in K)
$S$	Sutherland Constant
$k$	Thermal Conductivity
$C_p$	Specific heat capacity
$P_{inlet}$	Inlet Pressure
$P_{outlet}$	Outlet Pressure
$P_{gauge}$	Gauge Pressure
$P_o$	Stagnation Pressure in Settling chamber
$P_b/P_a$	Non-dimensional base pressure
$\sigma_k$	Turbulent Prandtl number
$\varepsilon$	Turbulent kinetic energy dissipation rate
$C_\mu$	Arbitrary Constant
$C_1$	Arbitrary Constant
$C_2$	Arbitrary Constant
$f_\mu$	Arbitrary Constant
$\sigma_\varepsilon$	Arbitrary Constant
$v$	Velocity
$\mu_t$	Turbulent Viscosity

$Pr_t$	Turbulent Prandtl number
L	Length of the enlarged duct
D	Diameter of the duct
W	Width of the rib
H	Height of the rib

## LIST OF ABBREVIATIONS

CFD	Computational Fluid Dynamics
NPR	Nozzle Pressure Ratio
TKE	Turbulent Kinetic Energy
BFS	Backward Facing Step
CD	Converging-diverging

# **SIMULASI CFD UNTUK MENGENAL PENGARUH GEOMETRI DAN KEDUDUKAN RUSUK DI DALAM ALIRAN MUNCUNG TUMPU PADA NOMBOR MACH SONIK**

## **ABSTRAK**

Kehadiran asas tumpul membawa kepada pemisahan aliran dalam badan aerodinamik, yang menyebabkan tekanan rendah di kawasan bangun. Pada nombor sonik Mach, tekanan rendah di kawasan bangun menyumbang sehingga enam puluh peratus daripada jumlah seret. Kajian ini dijalankan untuk mengkaji kesan rusuk segi empat tepat pada tekanan asas. Parameter yang dipertimbangkan adalah nisbah tekanan muncung, nisbah aspek tulang rusuk, Panjang kepada nisbah Diameter ( $L / D$ ) salur apabila diletakkan beralih dari subsonik ke nombor Mach sonik. Simulasi dilakukan menggunakan CFD, dan model turbulensi  $k-\epsilon$  digunakan. Pada mulanya, hasil simulasi yang diperolehi disahkan dengan kerja percubaan untuk nisbah  $L / D$  yang berbeza dari saluran pada pelbagai Numerik Tekanan Nozel (NPR), dan nisbah aspek tulang rusuk dari 3: 1 hingga 3: 3 untuk nisbah kawasan 6.25. Hasilnya dalam persetujuan yang baik dengan hasil eksperimen. Simulasi kemudian dilakukan untuk tulang rusuk tunggal, yang ditempatkan di pelbagai lokasi dan nisbah aspek untuk NPR dalam jarak antara 1.5 hingga 5 dari pangkalan. Variasi tekanan asas, halaju, dan perubahan medan untuk pembolehubah di atas dibincangkan. Keputusan simulasi menunjukkan bahawa tulang rusuk memecahkan vorteks utama di pangkalan dan membentuk pelbagai vorteks dan dengan itu mengawal tekanan asas di kawasan bangun. Keputusan menunjukkan bahawa rusuk segi empat tepat dengan nisbah aspek yang lebih rendah berkesan dalam mengurangkan tekanan asas, sedangkan rusuk dengan nisbah aspek yang lebih tinggi cenderung meningkatkan tekanan dasar. Simulasi juga dijalankan untuk saluran dengan garis pusat,  $D = 20$  mm. Dalam hal ini, tulang rusuk segi empat tepat dengan rasio aspek 3: 1, 3: 2, dan 3: 3 ditempatkan pada lokasi 20 mm, 40 mm,

60 mm, dan 80 mm, untuk NPR yang sama. Keputusan menunjukkan bahwa ketinggian dan lokasi tulang rusuk memainkan peranan penting dalam mengawal tekanan asas.

# CFD SIMULATION TO STUDY THE EFFECTS OF RIBS IN A CONVERGING NOZZLE FLOW AT SONIC MACH NUMBER

## ABSTRACT

The presence of a blunt base leads to flow separation in aerodynamic bodies, which causes a low-pressure in the wake region. At sonic Mach number, low pressure in the wake region contributes up to sixty percent of the total drag. This study is conducted to study the effect of the rectangular ribs on the base pressure. The parameters considered are the nozzle pressure ratio, rib's aspect ratio, Length to Diameter ( $L/D$ ) ratio of the duct when placed circumferentially operating from subsonic to sonic Mach number. The simulation is performed using CFD, and the  $k-\epsilon$  turbulence model is employed. Initially, the simulation results obtained are validated with experimental work for different  $L/D$  ratio of the duct at various Nozzle Pressure Ratio's (NPR), and the aspect ratio of the ribs from 3:1 to 3:3 for area ratio of 6.25. The results are in good agreement with the experimental results. Later simulations are done for a single rib, which is placed at different locations and aspect ratios for NPRs in the range from 1.5 to 5 from the base. Base pressure variations, velocity, and pressure field changes for the above variables are discussed. The simulation results indicate that the rib breaks the primary vortex at the base and form multiple vortices and hence controls the base pressure in the wake region. The results show that a rectangular rib with a lower aspect ratio is effective in reducing the base pressure, whereas the rib with a higher aspect ratio tends to increase the base pressure. The simulations are also conducted for a duct with a diameter,  $D = 20$  mm. In this case, the rectangular rib with aspect ratios 3:1, 3:2, and 3:3 is placed at 20 mm, 40 mm, 60 mm, and 80 mm locations, for the same NPRs. Results show that the height and position of the rib plays a vital role in controlling the base pressure.

# CHAPTER 1

## INTRODUCTION

### 1.1 Background

In the present world suddenly expanded flow find application in various areas like flow over a blunt projectile, supersonic parallel diffuser (for cruise correction), the engine of the jets and static testbed of rockets, the port of IC engine, vernier rocket and single expansion ramp nozzle (SERN) rockets. Sudden expansion relates to the internal backward-facing step, as shown in Figure 1.1. In an internal backward-facing step, flow separation may occur due to (1) increase in the area (The specific areas where the sudden expansion takes place are: blunt base of the shells, a backward-facing step, base of the fuselage of the aircraft/missile, where the pressure is sub-atmospheric) and (2) flow recirculation beneath the increased area. Reattachment point is a zone in which the shear layer will attach to the duct, and will start to grow.

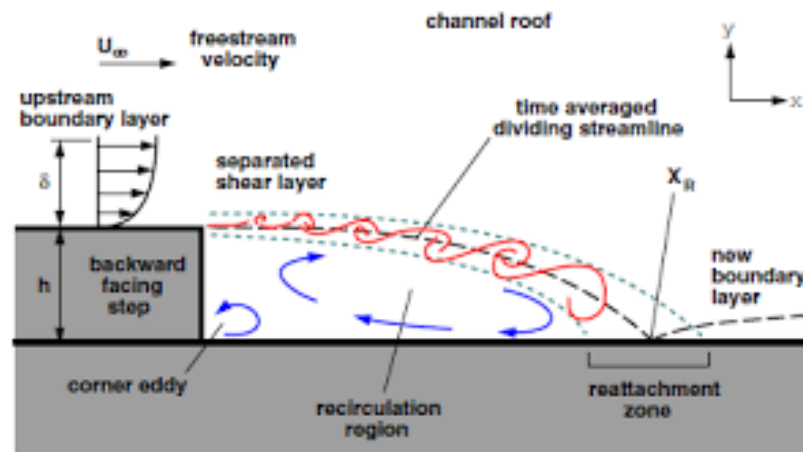


Figure 1.1: Backward Facing step (Saleel et al., 2013)

Hence, suddenly expanded flow that passed through the converging nozzle can be characterized by the flow separation, recirculation zone at the case corner, and reattachment of the stream. The separated flow is divided by the boundary layer into the



primary jet flow and the secondary flow recirculation region (Rathakrishnan, 2001). Under these circumstances, in the majority of the cases, the base pressure is sub-atmospheric, which is lower than the ambient pressure. This low pressure at the base corner results in high base drag. When the base drag is high, the range of the vehicle, rockets, bombs, missiles, and launch vehicles is reduced considerably hence become the main disadvantage of sub-atmospheric pressure at the base corner.

Application of separated flows can be found in many engineering problems such as the automobile industry, fuselage of aircraft, suddenly expanded pipes, combustors, diffusers, and turbines. Separated flow is mostly associated with the turbulence flow, and hence, there are many instabilities found in the stream. For decades many researchers have been working to understand the dynamics behind the instabilities of separated flow. Hussain (1986) documented the physics behind the instability in turbulent flow, and his findings motivated researchers in this field.

## **1.2 Problem Statement**

The recirculation zone formed at the base corners in missiles, projectiles, and rockets leads to flow separation in aerodynamic bodies, which causes a very low-pressure zone in the wake region of the base. This low base pressure results in a negative base pressure coefficient and hence a positive magnitude of the base drag. The base drag contributes to more than sixty percent of the total drag in any aerodynamic vehicle. Thus there is an urgent requirement to control this pressure and bring it close to atmospheric pressure.

The base drag reduction can be achieved by increasing the base pressure. This can be done by breaking the vortex in the recirculation zone. There are two ways to regulate the base pressure; (1) active control and (2) passive control. Dynamic control

requires blowing or suction methods; hence will need an external source of energy, which can be quite expensive. In some cases, it is not feasible to get an additional external source of energy. Whereas in the case of passive control, the base pressure can be controlled by geometrical changes in the flow field by employing ribs, cavities, boat tail, splitter plate, and locked vortex mechanism. Unlike active control, passive control does not require an external source of energy; hence, it is not expensive.

Earlier, sincere efforts were presented by the research community to control the base pressure and regulate/change the flow field using different methods. Quite interestingly, the entire set of works reported is purely experimental using microjets, ribs, or cavity. However, any kind of computational study on passive control of base pressure is not observed to figure out the minute details of flow phenomena occurring after the flow expansion. With this interest, ribs are used as passive control methods using a computational standard turbulence model and using ribs of different width to height ratio, except Rathakrishnan (2001), who has carried experimental investigation for different aspect ratio and NPR (nozzle pressure ratio). But the study is experimental, and the control being case sensitive, the trend obtained cannot be generalized. In order to achieve the best aspect ratio of the rib (width to height) and its appropriate location, an experimental investigation is not worthy, and understanding the physics is quite complicated. Since the reattachment location of the shear layer with the duct and hence, the magnitude of base pressure depends on the location of the rib and geometry of the rib. Therefore, this study aims to find the optimum position and geometry of the rib after validating the results of the reference paper. Hence, only one rib at different locations from 1D (diameter of the duct) to 4D with a different aspect ratio of ribs from 3:1 to 3:5 for various NPR in the range from 1.5 to 5 is considered in the numerical analysis.

### **1.3 Research Gap**

With many experimental works addressing the role of active control using micro-jets and other mechanisms, scope exists in controlling the base pressure using a passive control mechanism. Using ribs as passive control, except Rathakrishnan et al. (Rathakrishnan, 2001), no one has worked on this kind of control mechanism. The following gaps are further identified out of which the prime aim is to carry out the numerical analysis in this field of interest.

1. Understanding of fluid expansion in the duct affected by the presence of rib
2. Effect of single and multiple ribs on the base pressure and fluid field
3. Location and aspect ratio of the rib affecting the vortex formed and study of multiple vortices formed due to the presence of rib

### **1.4 Objectives of Research**

1. Verify experimental results using CFD.
2. To perform a parametric study by varying
  - (i) Number of Ribs.
  - (ii) Nozzle Pressure Ratio (NPR).
  - (iii) Location of Ribs.
  - (iv) Comparison between the area ratio

## 1.5 Scope of the Study

Figure 1.3 shows the features of a suddenly expanded flow from a converging nozzle exhausted into a circular duct which involves three fields of engineering problems, which are:

1. The vortex generation in the wake region at the base corner of the duct.
2. The dividing streamlines due to the flow separation while coming out from the nozzle. The point where it attaches to the duct is called the reattachment point.
3. The development of the boundary layer from the reattachment point, where the fully developed flow develops in the duct.

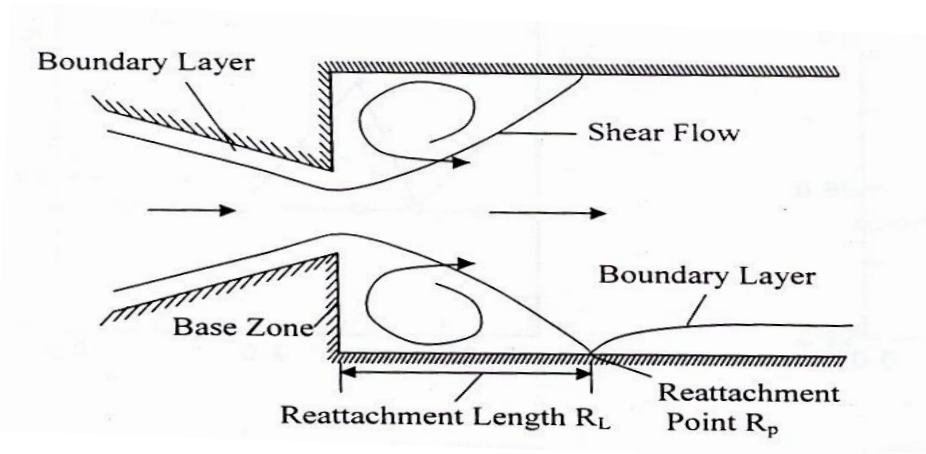


Figure 1.2: Suddenly Expanded flow (Ashfaq and Khan, 2014)

The present research focuses on the fluid dynamics aspect of the flow where the flow of fluid in the form of air through a converging nozzle discharged into a duct of a larger cross-sectional area is studied. The study covers the establishment of numerical simulations using Computational Fluid Dynamics (CFD), the validation through experimental work by Rathkrishnan (2001) who employed five ribs at 1D locations at various pressure ratios namely 1.141, 1.295, 1.550, 1.707 and 2.458, and

Mach number varied from subsonic to sonic. Through the CFD simulation, this study investigates further the effectiveness of the passive control methods in breaking the vortex by using the single rib of passive control at various aspect ratios, different L/D locations, and different Mach numbers from subsonic to sonic Mach numbers. Finally, the simulations are performed for area ratios of 4 and 6.25 with a single rib at various locations along the duct at a different level of expansion.

### **1.6 Contributions of this Research**

As this research is done using the Computational Fluid Dynamics (CFD) tool, we are able to observe the flow inside the duct and can visualize the various interesting phenomena happening inside the duct and then interpret the results accordingly. The outcome of this research can be beneficial for designing future aerospace vehicles.

### **1.7 Thesis Outline**

In order to understand the aim and objectives of this research, the thesis is written and compiled with the following chapters:

Chapter 1 presents the introduction of this study. This chapter presents the problem statement gap of knowledge, research objectives, and scope of the research.

Chapter 2 presents the state-of-the-art of the characteristics of the backward-facing step, applications of active control, merits, and demerits of dynamic control, advantages, and disadvantages of passive monitoring and its use in aerodynamics.

Chapter 3 discusses the methodology used in this research and the experimental method of the referenced paper. Also included is the numerical simulation of the flow field due to the sudden expansion in the area and the boundary conditions applied therein.

Chapter 4 presents the results and discussion. In this chapter, simulation results were compared with the experimental results. Contour plots of simulation results are shown. The base pressure results obtained from the simulation were validated with the experimental data.

Chapter 5 is about the conclusions drawn from this research and includes recommendations for future work.

## **CHAPTER 2**

### **LITERATURE REVIEW**

The importance of suddenly expanding fluid flow from nozzles has attracted numerous researchers to study this phenomenon in detail. The base pressure regulation using any kind of control is possible at a more significant rate. The literature review pertinent to control of base pressure is reviewed relevant to suddenly expanded flows. The study of investigations in the area of abruptly growing streams is divided based on active control and passive control. The flow expansion type is also considered for the literature review. These two subsections are further classified based on type Mach number. At first, we briefly introduce the importance of literature review in this field of base drag control, and then the analysis in the area of passive monitoring is provided to know the importance and their role played in control of base pressure.

#### **2.1 Characteristics of the Backward Facing Step**

We are considering the backward-facing step here as there exists a similarity between the backward-facing-step and suddenly expanded internal flow. As the backward-facing step is related to separated flow as when the flow separates from the wall, a wake region is created. In the downstream of the flow, the shear layer reattaches with the duct wall at a point, and this point is known as the reattachment point. A low-pressure wake region is created in which high-velocity recirculating bubbles rotate. The small vortices or coherent structures (Smits, 1981) in the shear layer rolls in and forms more prominent vortices with the primary vortex at the base corner. Besides the presence of coherent structures, recent studies (Chun and Sung, 1996, Roos and Kegelman, 1986, Sigurdson, 1995, Troutt et al., 1986) show that coherent structures

play a vital role in altering or controlling the base drag or fuel mixing in the combustion chamber or noise and vibrations.

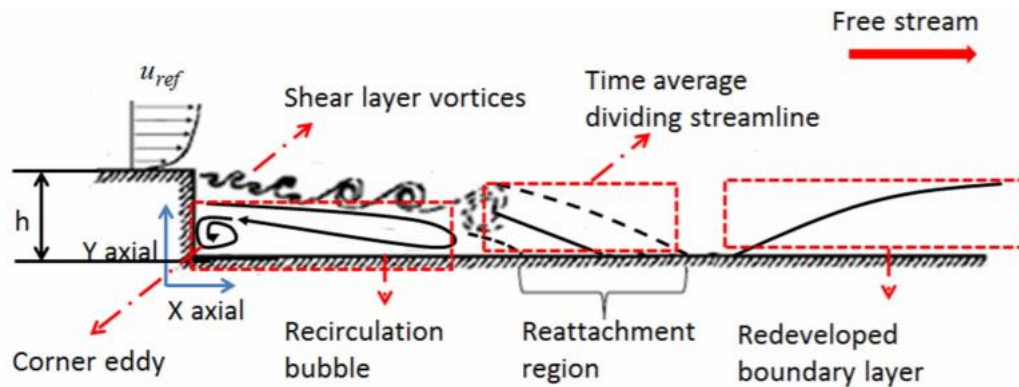


Figure 2.1: Flowfield at Backward Facing Step (Hsu and Lin, 2016)

The detail description of these characteristics is as given below:

### 2.1.1 Shear Layer

The shear layer is the layer that is accompanied by an adverse pressure gradient and change in the velocity among the adjacent layers, and this shear layer is highly viscous. The most common example of a shear layer is the flow over a solid, and that is termed as the boundary layer. This type of shear layer is found in BFS. The flow around the BFS is one of the complex flows, even though its geometry is simple. When the flow enters the nozzle, a shear layer is formed due to velocity difference, and at the exit of the nozzle, the flow separates and meets at one point, known as the reattachment point. The reattachment point is a variable in space due to the coherent vortices of the shear layer (Chun and Sung, 1996). According to Chandrasuda (Chandrasuda, 1975) and McGuinness (McGuinness, 1978), there is a movement of vortices due to the coherent shear layer into the recirculation zone due to the positive pressure gradient. The vortex will trigger the instability in the next shear layer; later, vortices will interact with the next shear layer.



Figure 2.1 shows the flow development at a backward-facing step with the shear layer. The recirculation zone is formed due to the decrease in the pressure and due to the reducing distance from the backward-facing step. As a result of this secondary vortex in the opposite direction are originated. From the literature, it is found that the length is 6 to 8 ( $L/D$  ratio) times that of the step height, as pointed out by Bradshaw and Wong (Bradshaw and Wong, 1972).

### 2.1.2 Coherent Structures

Coherent structures are a non-transient turbulent flow and are present in the stream for a relatively more prolonged period of time. The turbulent flow is a chaotic flow in fluid dynamics where the flow velocity gradient is substantial, and their trends are non-linear in both position and time. The *coherent structure* may be defined as a turbulent flow whose vorticity, which is usually stochastic, contains non-linear components.

Eddies are the ones with a circular motion and are present in the flow for a short duration of time. Whereas on the other side, coherent structures are the circular motion which persists for a more extended period of time and can be called as the vortex. Coherent structures have their own boundaries, and they are non-overlapping. In a BFS, it is noted that the eddies of the turbulent shear layer rolls-up and forms larger coherent structures.

Coherent structures are one of the most researched topics in the past few decades. These structures are present in the flows, such as turbulence in the form of boundary layers, jets, and wakes.

### **2.1.3 Reattachment Zone**

The reattachment zone comprises the separation point at which the flow separates due to the step height and meets at one point on the duct wall. This meeting point is called the reattachment point. From this reattachment point, the flow will grow again. The reattachment point is not fixed. The shear layer is an uncontrolled separating layer (Eaton and Johnston, 1982). The reattachment zone changes with time as it is not fixed and is associated with the high-frequency oscillations in the shear layer. These low-frequency oscillations are high in energy, as explained by many researchers (Eaton and Johnston, 1982; Farabee and Casarella, 1986; Liu et al., 2005, Roos and Kegelmann, 1986, Troutt et al., 1986). This unsteadiness in the shear layer is referred to as flapping. Strouhal frequency of this flapping phenomenon is found in many experiments as 0.2 (Kostas et al., 2002), Lee and Sung, 2001; Liu et al., 2005; Scarano and Riethmuller, 1999).

### **2.1.4 Recirculation Zone**

The recirculation zone is the region beneath the backward-facing step (BFS), which is enclosed by the unsteady shear layer and the wall of the duct. It consists of a bubble which recirculates to form the primary vortex, as shown in Figure 2.1. In view of the presence of the vortices in the unsteady shear layer, entrainment of the flow from the region into the recirculation zone occurs, thus creating a low-pressure recirculation region beneath the shear layer. The primary vortex formed consists of low circulatory velocity. The other significant vortex seen in this recirculation zone is the secondary vortex, which occurs at the corner of the step, which has opposite circulatory motion as the primary vortex.

The pressure at the blunt base of the artillery shell, the fuselage of an aircraft, and at the base of unguided rockets and missiles is sub-atmospheric. Hence, the subject of control of the base pressure has been of interest for the past many decades. Many researchers have tried to control the pressure at the base by employing both active and passive control techniques. In the past, researchers have used passive control techniques in the form of body boat-tailing (Mair, 1969, Maull and Hoole, 1967), base bleed (Bearman, 1967, Tanner, 1975, Wood, 1967), and various other vortex suppression (Pollock, 1969) devices are used to control the base pressure in missiles, projectiles or fighter planes. In order to control the base pressure, it is vital to break the vortex created at the blunt base of the rockets, shells, or automobiles.

Reducing the base drag in the context of two-dimensional flows are discussed in the papers by Nash (Nash, 1965) and Tanner (Tanner, 1975). Also, Mauri (Morel, 1978), Tanner (Tanner, 1975), and Murthy (Murthy, 1976, Murthy and Osborn, 1976) have written review papers on axisymmetric base drag reduction techniques in the past. They are cavities, step-bodies, boat-tail, and vortex locked mechanism.

The main reason behind the vortex generation and the ejection of mass, which leads to the backflow, was explained by Wicks (Khan et al.). The boundary layer is the source of two fluids, (1) recirculation zone and (2) backflow from the expanded section of the wall (Wick, 1953). Researchers, as discussed above, did research on the techniques of breaking the recirculation zone formed at the base and eventually controlling the base pressure.

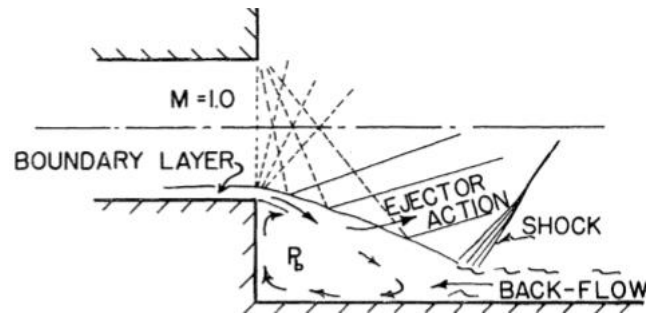


Figure 2.2: Jet-Pump action (Wick, 1953)

Figure 2.2 shows a formulated jet-pump action in which Wick explains about the boundary layer separation and its entrainment, backflow at the boundary layer edge, and the ejection action (Wick, 1953).

When the flow exits from a converging nozzle, the flow will be correctly expanded till  $NPR = 1.89$ . For NPR's more than 1.89, the flow will be under-expanded, and hence, there will be an expansion fan at the nozzle exit, through which flow will expand. Till the flow is choked, the exit pressure at the nozzle and the base pressure will be the same (i.e.,  $P_b = P_e$ ). The same has been observed by Wicks (1953).

There are two types of control techniques that are employed in order to control the base pressure, which is active control and passive control technique. The previous study on passive monitors on a different type of flow condition, namely subsonic flow, sonic flow, supersonic flow, will be discussed in detail.

Table 2.1: Types of Flow

Type of Flow	Description
1. Subsonic Flow	$0.6 \leq M \leq 0.9$
2. Sonic Flow	$M = 1$
3. Supersonic Flow	$1.2 \leq M \leq 4$
4. Under-expanded Flow	$P_e/P_{atm} > 1$

5. Correctly Expanded	$P_e/P_{atm} = 1$
6. Over-expanded Flow	$P_e/P_{atm} < 1$

## 2.2 Passive Control

Another method of controlling the base pressure is by applying inactive control. In the case of passive monitoring, the geometry is modified to attain the desired results. Various passive techniques available are cavities, ribs, boat-tail, and step body.

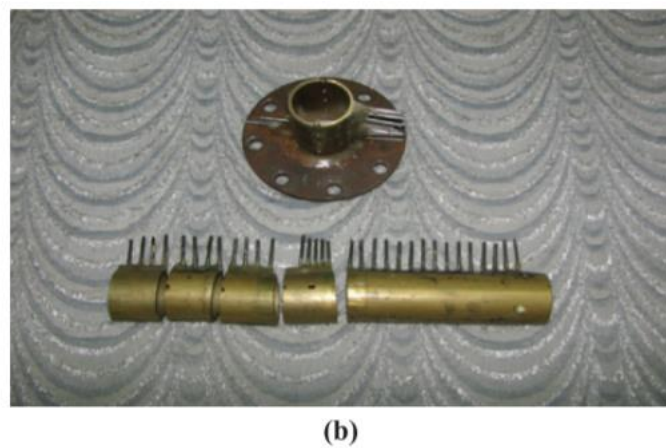
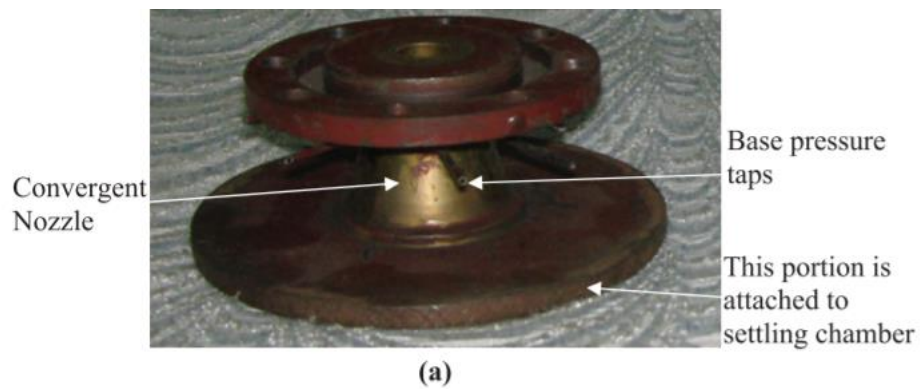
### 2.2.1 Applications of Passive Control in a Different Type of Flow

The passive control technique is of two types- one is in the form of ribs and others in the way of the cavity. Employing passive control techniques is inexpensive when compared to active control techniques.

#### a) Subsonic Flow

Rathakrishnan (2001) made use of passive control in the form of annular ribs. He used ribs with three aspect ratios, namely 3:1, 3:2, and 3:3. From his study, he concluded that rib with aspect ratio 3:1 gives the best result when compared to ribs 3:2 and 3:3. Ribs with aspect ratio 3:1 do not introduce any oscillations. The pressure loss in the duct is less than 6% when compared with the plain duct. Whereas 3:2 and 3:3 introduce mild oscillations and results in an increase of the base pressure. They concluded from their study that there is a limiting value for the rib aspect ratio in order to obtain the extreme suction at the base with the lowest pressure loss. Experimental Study by Vijayaraja et al. (Vijayaraja et al., 2014) on passive control in the form of annular ribs of aspect ratio ranging from 0.45 to 1.25 and NPR ranging from 1 to 7 was done. Based on their results, it was concluded that in the absence of rib in the plain duct, the flow is

intensely inclined by the NPR and L/D ratio of the enlarged duct. It was observed that for plain duct, the minimum L/D needed is  $L/D = 4$  for the flow to reattach with the duct wall and develop at subsonic and sonic conditions for area ratio 6.25. Whereas when compared with the enlarged duct with annular rib, it is perceived that till  $NPR = 3$ , there is either a slight growth or decline in base pressure. But for  $NPR \geq 4$ , the base pressure increases with the increase in NPR. Also, it is seen that the base pressure increases with the increase in the aspect ratio of the rib. Figure 2.3 shows the convergent nozzle, duct, and several annular ribs with a timber holder.



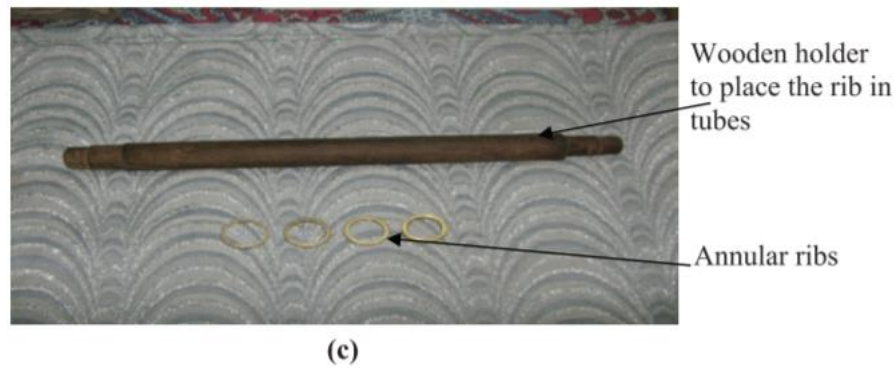


Figure 2.3: (a) Converging nozzle, (b) duct and (c) annular ribs with wooden holder (Vijayaraja et al., 2014)

M. Sundararaj et al. (Sundararaj et al., 2014) did a simulation of rectangular ribs of aspect ratio 3:1 and 1:1, semi-circular rib, triangular, and circular ribs. They found that the rectangular rib with aspect ratio 3:1 gives the most efficient result, and the annular rib is proved to reduce the base pressure when compared to the without rib case. They compared the simulation results with the experimental results and found that the results are in good agreement with the experimental results. Khan et al. (Khan et al., 2018b) did experimental as well as computational investigation on the effect of passive control in the form of dimples at different pitch circle diameters (pcd) in order to control the base drag in subsonic suddenly expanded flow. From their research, they concluded that dimple helps in controlling base drag by increasing the base pressure. Also, as the length of the duct increases the control becomes more effective. Hence, for a given Mach number and  $L/D$  ratio, one can identify the optimum  $L/D$  ratio of the duct, which will result in a maximum increase or decrease of base pressure.

Figure 2.4 shows the dimensions of the nozzle used for the experiments.

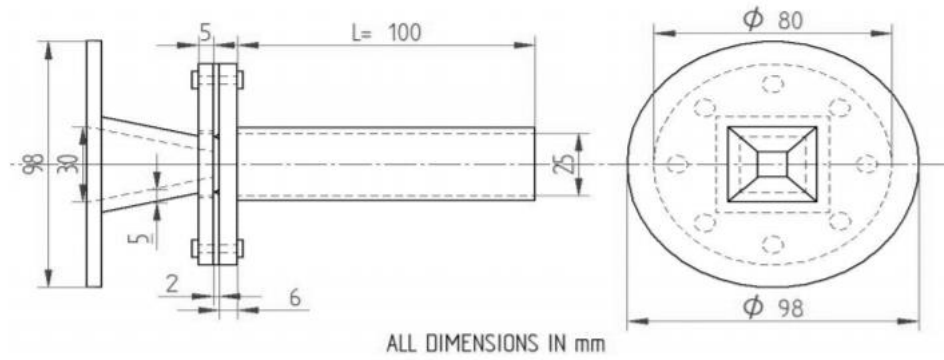


Figure 2.4: Nozzle and duct dimensions (Khan et al., 2018b)

Khan et al. (Khan et al., 2018c) did the experimental investigation to compare the influence of multiple cavities for duct lengths of  $4W$ ,  $6W$ , and  $8W$ . It was observed that the multiple cavities are very useful in controlling the base pressure. Additionally, it becomes more effective as the duct length increases. Wall pressure is not affected by the use of multiple cavities for the duct length  $6W$  and  $8W$ . However, for the  $4W$ , the wall pressure is unpredictable and is associated with the oscillations. Hence, for a given Mach number, one can identify the optimum  $L/D$  ratio of the duct, which will result in an extreme growth/decline of the base pressure. Aravind and Al-Garni (Aravind and Al-Garni, 2009) did an experimental investigation of the effect of base cavities on the base pressure and wake of a two-dimensional bluff body. In their results, they presented results of a preliminary study to determine the effects of base cavities on the base pressure and wake behind a two-dimensional bluff body. The bluff body model has an elliptical leading edge with an axis ratio of 8:1 and a blunt base. Experiments were conducted at a Reynolds number based on the height of the model,  $Re_h$ , of  $2.6 \times 10^4$ . Steady base pressures at several pressure ports along the spanwise length of the model as well as Particle Image Velocimetry (PIV) data of the near-wake velocity fields behind the reference model and base cavities were obtained. The steady base pressure measurements show that base pressure increases with the attachment of the cavities.



The highest increase is 46% for the  $1/3 h$  cavity. The PIV measurements show two recirculation regions in the near wake of the base model as well as the cavities. They also show that the mean flow field and the lengths of the recirculation regions are not altered or affected much by the presence of the cavities. Jeff Howell et al. (Howell et al., 2012) studied bluff body drag reduction with ventilated base cavities. In their research, they presented Various techniques to reduce the aerodynamic drag of bluff bodies through the mechanism of base pressure recovery have been investigated. These include, for example, boat-tailing, base cavities, and base bleed. In this study, an Ahmed body in the square back configuration is modified to include a base cavity of variable depth, which can be ventilated by slots. The investigation is conducted in freestream and in ground proximity. It is shown that, with a plain cavity, the overall body drag is reduced for a wide range of cavity depths, but a distinct minimum drag condition is obtained. On adding ventilation slots, a comparable drag reduction is achieved but at a significantly reduced cavity depth. Pressure data in the cavity is used to determine the base drag component and shows that the device drag component is significant. Modifications of the slot geometry to reduce this drag component and the effects of slot distribution are investigated. Some flow visualization using PIV for different cavity configurations is also presented. Wagner et al. (Wagner et al., 2013) did an experimental investigation of aspect-ratio effects in transonic and subsonic rectangular cavity flow. In their research, Experiments were conducted at freestream Mach numbers of 0.55, 0.80, and 0.90 in open cavities having a length to depth ratio  $L/D$  of 5. The boundary layer at the cavity entrance was turbulent with a thickness of about  $0.5 D$ . The length to width ratio  $L/W$  was varied between 1.00, 1.67, and 5.00. Two stereoscopic PIV systems were used simultaneously to characterize the flow along the streamwise –wall-normal symmetry plane. The recirculation region was weakest in the  $L/W = 1.67$  flow,

a trend previously observed at supersonic Mach numbers. The  $L/W = 1.00$  cavity had the highest turbulence intensities and aft-wall pressure fluctuations. The two narrower cavities exhibited lower turbulence intensities and lower pressure fluctuations of a comparable level. The narrowest cavity exhibited the most significant spanwise coherence at the fore and aft walls; an observation possibly related to reduced spanwise flow in comparison to the broader cavities. Simultaneous pressure data showed the narrowest cavity to have modes two and three active for all Mach numbers. However, despite similar mean and turbulence fields, the  $L/W = 1.67$  sound pressure level spectra varied significantly with the Mach number.

Cai and Chung (Cai and Chng, 2009) studied on vortex shedding from bluff bodies with base cavities. In an extension of their previous drag reduction study via geometric shaping, this paper describes a numerical study of a quasi streamlined body in which the trailing edge is modified to form a base cavity. Here, they seek to establish if any synergistic merits exist through a combination of a spanwise wavy trailing edge with a straight-edged base cavity. Both two-dimensional and three-dimensional 3D simulations are conducted to assess the effect of Reynolds number, streamwise cavity length, and spanwise waviness on the flow. Two-dimensional simulations examining a variation in Reynolds number for a cavity of constant length reveal the presence of three different general wake patterns: the steady wake, the Karman wake, and an asymmetric, deflected wake. Most critically, the origins of the deflected wake pattern are traced to the presence of a vortex which resides within the base cavity. Similarly, for a constant Reynolds number, the influence of the cavity length on the flow is also intricately related to this cavity vortex, giving rise to wake topologies that bear a strong resemblance to the above three shedding processes. Reductions in drag are observed for all the investigated cavity configurations, and additionally, it is found that the magnitude of

the reduction obeys a direct relationship with the length of the cavity up to a particular asymptotic value. The results of the 3D simulations reveal that the current base-cavity arrangement appears to yield potential for further reduction in form drag as compared to earlier studies where the entire base region is modified in the shape of a wave. However, for a fixed cavity length, introducing spanwise waviness reduces the fluctuation intensity of the form drag but offers no obvious added benefit in terms of the time-averaged values. They anticipate that the presence of the straight-edged cavity causes a loss of spanwise coherence of these structures such that further enhancements due to the introduction of waviness are of less consequence.

#### **b) Supersonic Flow**

Mc\_Cormick (McCormick, 1993) made an experimental comparison on the two passive control techniques, namely low-profile vortex generator and a cavity generator. He found the advantages and disadvantages of both the passive control systems and gave the application of both the passive control system. Alam et al. (ALAM, 2007) did a computational investigation for supersonic two-dimensional flow where a square cavity was created to control the oscillations in free streamflow. It was observed from their study that the oscillations were high in the without control case, whereas in the presence of control case, the oscillations were low not only in the region of the main flow in axisymmetric nozzle but also inside the cavity.

### **2.2.2 Advantages of Passive Control**

The experiments were conducted through passive control methods that are very easy/simple and cost-effective. The passive control requires only geometrical changes

in the flow geometry. The main advantage of passive monitoring is that it does not require a new source of energy to operate the control mechanism.

### **2.2.3 Disadvantages of Passive Control**

Passive control does not have control over the generation of noise and vibrations. Since the cause of the signal is beyond the control of the evaluator. Because inactive fields are usually the result of assimilating exceptional geologic contributions over vast areas, documentation of the cause of an abnormal evaluation can be challenging. One or two fixed field ways are customarily used. This confines the extent of customization that can be completed for a given problem. The data sets observed in passive experimentations are lesser than those acquired in experimentations by active control and usually do not allow for detailed information and clarification.

### **2.3 Summary**

From the above review, it is evident that passive control is the most effective way to control the base pressure and hence the base drag. In passive control, there is no need for any external source of energy. The external source energy requirement for active monitoring is the most pressing problem to address. Hence, the majority of researchers prefer to employ passive control instead of dynamic control. From the literature, it is found that whenever the flow exiting from the nozzle is under expanded, the flow undergoes expansion, resulting in the formation of the barrel shock and the triple point.

From various literature resources, most importantly to be noticed is the comparative analysis of research works performed on the active control of different Mach flows. To be in brief, Khan et al. (Khan and Rathakrishnan, 2003), Khan et al.

(Khan and Rathakrishnan, 2006), Rehman et al. (Rehman and Khan, 2008), Baig et al. (Baig et al., 2012a), Baig et al. (Baig et al., 2012b), Pathan et al. (Pathan et al., 2018), Khan et al. (Khan et al., 2018a), Pathan et al. (Pathan et al., 2019), and others experimented with reducing the base drag using active control mechanism. The differences lie in consideration of Mach number for their study. However, sonic number study are least to report in the area of active and passive control of pressure drag. Thus the motivation of this work is to address the impact of ribs as passive control at sonic Mach number on the variation of base pressure using computational fluid dynamics approach.

In view of the above discussion, it is seen that in literature, people have conducted experiments using passive methods like cavities, ribs, step-body, boattail, and vortex-locked mechanism. However, to the best of our knowledge, no study has been done using CFD for sonic Mach numbers. Hence, the present study is an attempt to numerically simulate the suddenly expanded flow from the converging nozzle using a single rib at various locations and the NPR for two area ratios, namely area ratio 6.25 and 4, respectively.

## **CHAPTER 3**

### **METHODOLOGY**

#### **3.1 Introduction**

In this chapter, the procedure of the research is presented. The chapter is divided into four sections. The first section provides the governing equations used in the simulation. In the second section, the establishment of the CFD simulation is performed, and the validation with the previous work is compared. In the third section, the set up for duct of diameter,  $D = 25$  mm, is briefly explained, and finally, the set up for the pipe of diameter,  $D = 20$  mm, is defined in the final section.

Figure 3.1 shows a flowchart that represents an overview of the whole method performed in this study.

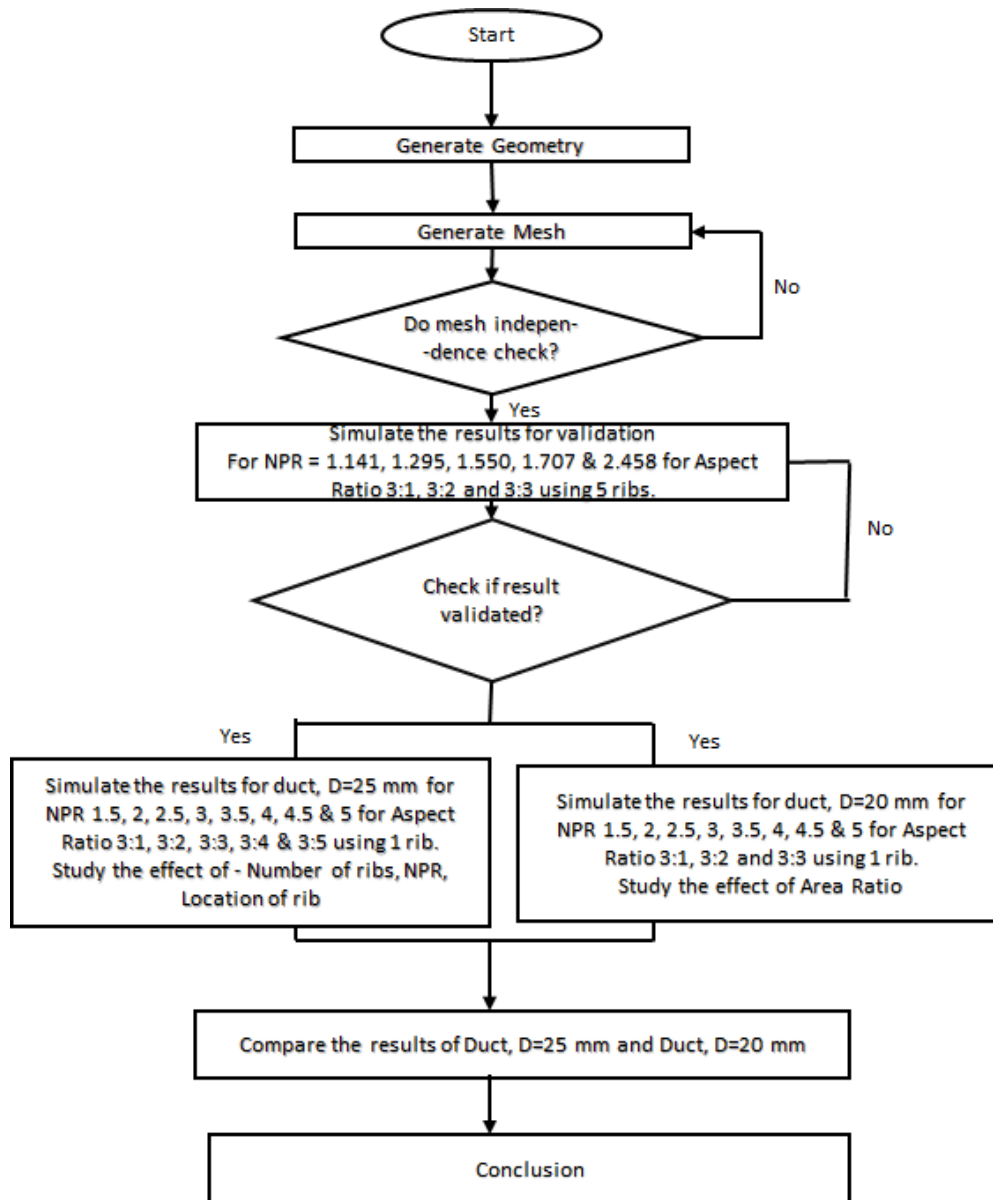


Figure 3.1: Flowchart for the layout of research

### 3.2 Governing Equations Related to the Simulation

The numerical modeling deals with the selection of proper mathematical models, i.e., governing equations, boundary conditions, the mesh quality, and the numerical scheme to solve the governing equations simultaneously. Although the computational method does not represent physical phenomena precisely, it provides sufficiently an insight into the flow behavior and is trusted over decades. Therefore, this requires a proper selection of aspects that can closely mimic the flow behavior. In this work, the